Experimental transient natural convection heat transfer from a vertical cylindrical tank

José Fernández-Seara, Francisco J. Uhía, J. Alberto Dopazo

Accepted Manuscript

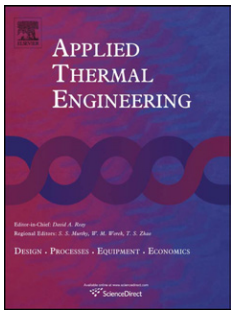

Title: Experimental transient natural convection heat transfer from a vertical cylindrical tank

Authors: José Fernández-Seara, Francisco J. Uhía, J. Alberto Dopazo

PII: S1359-4311(11)00119-0

DOI: 10.1016/j.applthermaleng.2011.02.037

Reference: ATE 3449

To appear in: *Applied Thermal Engineering*

Received Date: 3 January 2011

Revised Date: 16 February 2011

Accepted Date: 20 February 2011

Please cite this article as: J. Fernández-Seara, F.J. Uhía, A. Dopazo. Experimental transient natural convection heat transfer from a vertical cylindrical tank, Applied Thermal Engineering (2011), doi: 10.1016/j.applthermaleng.2011.02.037

EXPERIMENTAL TRANSIENT NATURAL CONVECTION HEAT TRANSFER FROM A VERTICAL CYLINDRICAL TANK

José Fernández-Seara, Francisco J. Uhía, J. Alberto Dopazo

Área de Máquinas y Motores Térmicos. E.T.S. de Ingenieros Industriales. University of Vigo.

Campus Lagoas-Marcosende 9, 36310 Vigo, Spain

*Corresponding author: Prof. José Fernández-Seara

E-mail: jseara@uvigo.es

Tel.: +34 986 812605

Fax: +34 986 811995

Abstract

In this paper heat transfer experimental data is presented and compared to general correlations proposed in the literature for transient laminar free convection from a vertical cylindrical tank. The experimental data has been obtained from heating and cooling experiments carried out with a cylindrical full-scale hot water storage tank working under real operating conditions. The experimental device and the data acquisition system are described. The calculation procedures established to obtain the experimental values of the heat transfer coefficients, as well as the data reduction process, are detailed. The local convection and radiation heat transfer coefficients are obtained from different heating power conditions for local Rayleigh numbers within the range of $1x10^5$ to $3x10^8$. The great quantity of available experimental data allows a detailed analysis with a reliable empirical base. The experimental local convection heat transfer coefficients are correlated and compared to correlations proposed in open literature for engineering calculations.

Keywords: transient convection coefficient, natural convection, vertical cylinder, hot water storage tank

Nomenclature

A	area	m^2
Cp	specific heat capacity at constant pressure	$J \cdot kg^{-1} \cdot K^{-1}$
di	inner diameter	m
de	outer diameter	m
Fo	Fourier number	
g	gravity acceleration	$m \cdot s^{-2}$
Gr	average Grashof number based on cylinder height	
Gr_x	local Grashof number at height x from bottom	
H	vertical cylinder height	m
h_x	local heat transfer coefficient	$W \cdot m^{-2} \cdot K^{-1}$
k	Thermal conductivity	$W \cdot m^{-1} \cdot K^{-1}$
Nu	average Nusselt number based on cylinder height	
Nu_x	local Nusselt number at height x from bottom	
Pr	average Prandtl number	
Pr_x	local Prandtl number at height x from bottom	
Ra	average Rayleigh number based on cylinder height	
Ra_x	local Rayleigh number at height x from bottom	
q	heat flow rate	W
q'	heat flow rate per unit length	$W \cdot m^{-1}$
q"	heat flux	$W \cdot m^{-2}$
ri	inner radius	m
ro	outer radius	m
t	time	s
T	temperature	K
U	overall heat transfer coefficient	$W \cdot m^{-2} \cdot K^{-1}$
x	height from the base of the cylinder	m, mm
y	distance between temperature sensors inside the tank	m, mm

Greek symbols

α	fluid thermal diffusivity	$m^2 \cdot s^{-1}$
β	fluid thermal expansion rate	K^{-1}
ε	surface emissivity	
μ	dynamic viscosity	$kg \cdot m^{-1} \cdot s^{-1}$
v	kinematics viscosity	$m^2 \cdot s^{-1}$
ρ	density	$kg \cdot m^{-3}$
σ	Stefan-Boltzmann constant	$5.67 \bullet 10^{-8}$ $W \cdot m^{-2} \cdot K^{-4}$

Subscripts

a	surrounding air
cv	convection
f	film
i	inner
ins	insulation
ms	metal sheet
o	outer
s	outer cylindrical surface
t	tank
rd	radiation
w	wall
x	local, related to height
wt	water
∞	ambient

1. INTRODUCTION

Different heat transfer textbooks and manuals present empirical correlations for natural convection heat transfer involving a great variety of geometries [1, 2]. These correlations usually account for steady-state processes and comprise cases of either constant surface temperature or constant heat flux. However, in practice, none of these theoretical cases normally occurs and the steady-state correlations provide an inaccurate approach to the real data.

Therefore, the analysis of practical transient heat transfer problems as well as the contrast between actual results obtained in practice and results provided by correlations commonly used by engineers is an interesting matter that can help commitments to be made based on the accuracy of the calculations.

Transient natural convection between a surface and a fluid exits either when the wall temperature or the fluid temperature changes. In practice, the free convection processes take place in numerous applications of heating and cooling of a body immersed in a fluid. In such processes neither the surface temperature nor the heat flux are not usually constant or change in a systematic way.

The interaction between tanks used for storing energy and the surrounding ambient is a common transient heat transfer application. In these tanks, heat is transferred by transient natural convection and radiation from its outer surface to the surroundings. The tank wall and the ambient temperature generally change during both the heating and cooling processes.

The transient natural convection heat transfer has been studied by several authors. Siegel [3] analyzed the boundary layer growth when a semi-infinite vertical plate was subjected to step heating and described three different conditions in function of time frames. For short periods, the local heat transfer is produced mainly by conduction heat transfer mode, for longer periods steady-state conditions can be applied and for intermediate periods, the local heat transfer coefficient directly depends on time. Goldstein and Eckert [4] validated these results experimentally. Gebhart [5, 6] studied the transient regimen for vertical plates and cylinders

paying special attention to the thermal capacity effect of the wall. Churchill [7] proposed a general correlation for free convection from a vertical plate following a step in heat flux density for all times, Pr>0.01 and all Ra in the laminar boundary layer regime. This last correlation is still proposed in practice to be used in heat exchanger design [8].

In recent years, Harris et al. [9] obtained an analytical solution for the transient free convection from a vertical plate when the plate temperature is suddenly changed. Maranzana et al. [10] studied experimentally the transient free convection heat transfer coefficient on a vertical flat plate with different levels of heating immersed in air. Their results showed that for short periods, the transfer coefficient decreases proportionally to t^{-1} and not to $t^{-1/2}$ as the conduction theory had anticipated. De Lorenzo and Padet [11] investigated how free convection heat transfer can be optimised when a periodical heat flux density is applied to a vertical surface. Saeid [12] studied the effect of the periodic oscillation of the surface temperature on transient free convection from a vertical plate. Shapiro and Federovich [13] analyzed the Prandtl number dependence of unsteady natural convection along a vertical plate in a stable stratified fluid. Lin et al. [14] evaluated the transient natural convection boundary-layer flow adjacent to a vertical plate heated with a uniform flux in an initially linearly-stratified ambient fluid with Prandtl numbers less than one by using scaling analysis and direct numerical simulation.

The purpose of this research is two fold. On one hand to supply actual data of a natural heat transfer process from a real practical engineering application, and on the other hand to figure out the approximations and discrepancies between theoretical results obtained from well-known correlations available for engineering calculations and an actual and common heat transfer process in the reality.

In the paper, the experimental set up used to obtain the experimental data is described. The calculation procedure established to determine the local transient convection heat transfer coefficients and the dimensionless data analysis is explained. The results of the experimental data compared to the data obtained from available correlations are shown. Moreover, a general

form for a correlation is proposed and the numerical coefficients are obtained correlating the available experimental data.

2. EXPERIMENTAL DEVICE

The experimental data reported in this paper has been taken from an experimental device that is being used for a more general study to characterize the thermal behaviour of actual and full-scale hot water storage tanks. The experimental set-up consists of a vertical cylindrical hot water storage tank provided by the Spanish manufacturer Galifar. The tank is made of stainless steel and a cylindrical cover made of a carbon steel sheet. The thermal conductivity of the outer metal sheet is 50 $W \cdot m^{-1} \cdot K^{-1}$, the thickness 1 mm and is externally white lacquer. The space between the tank and the external cylindrical cover is filled with injected polyurethane foam with thermal conductivity of 0.028 $W \cdot m^{-1} \cdot K^{-1}$. The external shape of the tank is a perfect cylinder of 546 mm in diameter and 1010 mm in height. The commercial tank is equipped with an electric heater of 2.2 kW located vertically in the bottom. In this experimental work, an electric heater composed of three equal elements with an electric power of 4 kW each, which can be turned on/off independently, has also been used. The height of both heating elements is 360 mm. The tank is placed vertically elevated on a platform. The external shape of the tank and its transversal section are schematically depicted in figure 1, including the values of the significant dimensions for the natural convection heat transfer analysis. The natural heat transfer processes from the outer cylindrical surface of the tank to the surroundings have been performed considering a long cylinder. The influence of the plain bottom and top covers is neglected.

The experimental device has been equipped with an acquisition data system based on a PC with a data acquisition card. The water temperature distribution inside the tank is measured by using nine temperature sensors distributed uniformly along the height of the tank. The separation between them is 80 mm. All water temperature sensors are situated at 160 mm from the tank vertical axis (s_w in figure 1). These temperature sensors are A Pt100 inserted in 200 mm long and 6 mm diameter stainless steel pockets. The temperature on the outer cylindrical

surface of the tank is measured by means of three A PT100 sensors attached directly on the external tank surface (s_t in figure 1). A hole has been made through the external cover and the insulation, the external surface of the tank carefully cleaned, and the sensor attached in good thermal contact with the outer tank surface. Once the sensor has been placed, the hole was filled with the same type of insulation. These sensors are separated at 320 mm intervals in such a way that their positions coincide in height with sensors which measure the water temperature inside the tank, but are set at an angle of 45º to them. Three A PT100 sensors also measure the temperature on the outer cylindrical surface (s_s in figure 1). These sensors have been placed at the same heights as the sensors attached to the tank surface but set at an angle of 22.5º to them, as shown in figure 1. The ambient temperature is measured by using two A PT100 sensors placed 500 mm apart from the tank at heights corresponding to its bottom and top. The characteristic ambient temperature is calculated by averaging the measurements of both sensors. The data acquisition system continuously sampled and recorded the temperature in each sensor at time intervals of 15 seconds. Then, the time temperature distributions on the outer surface of the tank and on the outer cylindrical surface at heights of 210 mm, 530 mm and 850 mm from the bottom, as well as the ambient temperature, are recorded in the corresponding data files.

The calibration test of the data acquisition system shows that the average error in temperature measurements is within ±0.2 K.

3. EXPERIMENTAL PROCEDURE AND DATA REDUCTION

3.1. Experimental procedure

Initially several tests were performed in steady-state conditions with water temperatures at the middle of the tank within the range of 313.15 to 343.15 K (40 to 70 ºC), with 5 K temperature steps, for the experimental procedure validation. Each test was repeated three times for each water temperature considered. Taking into account that the ratio “diameter/ height” is large at the three measurement positions experimentally evaluated, the local free convection heat transfer coefficient for the vertical cylinder storage tank can be calculated as the convection

heat transfer coefficient from a vertical flat plate with the same height by using well-known correlations found in open literature. In this case, the condition calculated in Eq. (1) was satisfactory for all the tests performed.

$$\frac{de}{H} \geq \frac{55}{Gr_x^{1/4}} \qquad (1)$$

Subsequently, transient heating and cooling processes were evaluated in water storage tank's static operation mode. They were carried out with heating powers of 2.2, 4 and 12 kW, and at water atmospheric pressure. Before each heating process, the tank was fully filled with water at ambient temperature. The laboratory room was then emptied and locked, and a ten minutes waiting period observed to allow any air disturbance within the laboratory to calm down. The laboratory is subject to ambient temperature variations. The heating process starts when the electric heater is turned on and finishes when the water temperature at the middle of the tank reaches the set value of 353.15 K (80 ºC). Then, the electric heater is turned off and the cooling period begins. The experiment finishes when the water temperature in the tank is below 313.15 (40 ºC), this being considered, in practice, the minimum useful water temperature. The data acquisition system continuously recorded the temperature values measured by each sensor from the beginning to the end of the experiment.

3.2. Data reduction

A calculation procedure was established taking into account the experimental device characteristic data, geometry (depicted in figure 1) and the temperatures measured experimentally by the sensors whose positions are also shown in figure 1. The thermal emissivity proposed in open literature for the outer cylindrical surface finish (white lacquer) is within in a range of 0.88 to 0.96. In this research the outer surface thermal emissivity was determined experimentally by using a non contact multi-band method [15]. Experimental results showed an emissivity value of 0.92.

The calculation procedure was applied to the tank transversal sections at heights of 210 mm, 530 mm and 850 mm corresponding to the x_1, x_2 and x_3 positions (see figure 1) of the temperature sensors. The transient local convection heat transfer coefficients at those heights are obtained as described below.

The calculation procedure is based on an energy balance on the outer cylindrical surface of the tank at each one of the transversal section corresponding to the three heights considered in the analysis. The heat transfer from the outer cylindrical surface to the ambient is due to convection and radiation transfer, according to Eq. (2). The convective and radiative heat fluxes are calculated respectively in Eq. (3) according to Newton´s law of cooling, and in Eq. (4).

$$q''_{x,t} = q''_{x,cv} + q''_{x,rd} \qquad (2)$$

$$q''_{x,cv} = h_x \cdot (T_{x,s} - T_a) \qquad (3)$$

$$q''_{x,rd} = \varepsilon \cdot \sigma \cdot (T_{x,s}^4 - T_a^4) \qquad (4)$$

The total heat flux that reaches the outer surface of the metal sheet from the outer surface of the tank at each section is calculated taking into account that it is transferred by conduction through the insulation and the metal sheet. Eq. (5) gives the heat flux referred to at the outer surface of the metal sheet.

$$q''_{x,t} = \frac{T_{x,t} - T_{x,ms}}{r_{o,ms} \cdot \left[\frac{ln\left(\frac{r_{i,ms}}{r_{o,t}}\right)}{k_{ins}} + \frac{ln\left(\frac{r_{o,ms}}{r_{i,ms}}\right)}{k_{ms}} \right]} \qquad (5)$$

Taking into account Eqs. (2) to (5) and an energy balance at the outer surface of the metal sheet, the convection heat transfer coefficient is obtained in Eq. (6). Moreover, Eq. (7) gives the radiative heat transfer coefficient, which corresponds to the second term on the right-hand side of Eq. (6).

$$h_{x,cv} = \frac{1}{r_{o,ms} \cdot (T_{x,ms} - T_a)} \cdot \frac{T_{x,t} - T_{x,ms}}{\frac{ln\left(\frac{r_{i,ms}}{r_{o,t}}\right)}{k_{ins}} + \frac{ln\left(\frac{r_{o,ms}}{r_{i,ms}}\right)}{k_{ms}}} - \varepsilon \cdot \sigma \cdot \frac{T_{x,ms}^4 - T_a^4}{T_{x,ms} - T_a} \quad (6)$$

$$h_{x,rd} = \varepsilon \cdot \sigma \cdot \frac{T_{x,ms}^4 - T_a^4}{T_{x,ms} - T_a} \quad (7)$$

According to the calculation procedure exposed above, the transient convection heat transfer coefficient and the radiative heat transfer coefficient are calculated at three different heights corresponding to the sections where the temperatures are experimentally measured. Then, the time distributions of the local heat transfer coefficients are obtained. The analysis was based on the dimensionless numbers commonly used in natural convection processes to data reduction. The local Nusselt, Prandtl and Rayleigh numbers are calculated according to Eq. (8), (9) and (10), respectively. The data reduction calculations were effected by means of a spreadsheet. The air properties are evaluated at the mean film temperature by using the Refprop Database [16] incorporated into the calculation sheet as a dll.

$$Nu_x = \frac{h_{cv} \cdot x}{k_x} \quad (8)$$

$$Pr_x = \frac{Cp_x \cdot \mu_x}{k_x} \quad (9)$$

$$Ra_x = \frac{g \cdot \beta_x \cdot (T_{x,ms} - T_\infty) \cdot x^3}{\nu_x \cdot \alpha_x} \quad (10)$$

4. RESULTS AND DISCUSSION

4.1. Experimental data validation

Figure 2 shows experimental steady-state process results for the local Nusselt number at the three heights evaluated. Data for laminar regimen ($Ra<10^9$) and steady-state conditions from Eq. (11) of Churchill and Ozoe [17] for a uniform heating vertical plate and from Eq. (12) of Churchill and Chu [18] for isothermal vertical plate are included. These correlations are applicable for the vertical cylinder storage tank considered in this research that satisfies the condition expressed in Eq. (1).

$$Nu_x = \frac{0.563 \cdot Ra_x^{1/4}}{\left[1+\left(\frac{0.437}{Pr_x}\right)^{9/16}\right]^{4/9}} \qquad (11)$$

$$Nu_x = 0.68 + \frac{0.503 \cdot Ra_x^{1/4}}{\left[1+\left(\frac{0.492}{Pr_x}\right)^{9/16}\right]^{4/9}} \qquad (12)$$

In figure 2 it can be appreciated that the experimental results for the local Nusselt number concur with the Churchill and Ozoe correlation's data for uniform heating of a vertical plate, within the range for the local Rayleigh number from $1x10^6$ to $3.2x10^8$. The deviation observed was less than ±5%. On the other hand, the Churchill and Chu correlation's data for isothermal vertical plate underestimates the local Nusselt number by about 12.5%. Taking into account these results it can be inferred that the experimental procedure described above can be accepted for the investigation of the transient local free convection heat transfer coefficient on the external surface of the vertical cylinder storage tank.

4.2. Transient heating process

For the kind of heating processes considered in this analysis, the outer cylindrical surface temperature, the surrounding air temperature and the heat transferred from the tank to the surroundings do not remain constant during the process. In addition, the outer surface temperature depends on the height of the tank because of the water temperature stratification that occurs on its inside. Taking into account these considerations, the transient behaviour of the processes can be explained directly as a function of the outer cylindrical surface-surrounding air temperature differences, instead of time. Time dependence is also included in the local Rayleigh number through the temperature difference that appears in it's definitions (Eq. 10). Results for temperature differences less than 0.2 K have been neglected in line with the average error in temperature measurements observed from the data acquisition system calibration test performed.

Figure 3 depicts the experimental results for local convection and radiation heat transfer coefficients as a function of the temperature difference between the outer surface and surrounding air. The outer surface temperature ranged from 297.47 to 310.63 K and the surrounding air temperature varied from 296.68 to 304.12 K. In figure 3, it can be appreciated from the middle and top positions (x_2 and x_3 in figure 1) that the local convection coefficients are similar at each time step while the local convection coefficients determined at the bottom position (x_1) are higher. This can be explained because of the water temperature distribution inside the tank, as a result of the water temperature stratification phenomena. The water temperature stratification in the storage tank evaluated in the present study was analyzed in a previous research developed by Fernández-Seara et al. [19]. Their experimental results showed that at the upper half of the tank the water temperatures measured at different layers were similar whilst in the lower half of the tank temperature gradients were observed amongst the waters layers.

In addition, in figure 3 it can be observed that the convection coefficient at the three measurement positions can be approximated to a single asymptotical function, which seems to indicate that the transient behaviour of the local convection coefficient is highly dependent on the evolution of temperature differences during the process, as was expected. This behaviour

was observed for the three heating powers evaluated in this research as shown in figure 4. In the figure, the highest experimental data dispersion was observed for the fastest heating process, which corresponds to heating power of 12 kW.

On the other hand, figure 3 shows that the radiation heat transfer coefficient remains fairly constant during the process. The radiation coefficients were similar at the three measurement positions for each temperature difference value. These instantaneous values of the radiation coefficients form a straight line in figure 3 with values around 5 $W \cdot m^{-2} \cdot K^{-1}$.

Furthermore, figure 3 shows that for temperature differences of 0.3 K or lower the convection coefficient tends to rise a lot and the radiation coefficient tends to be negligible compared to the convection coefficient. As the temperature difference increases, the convection coefficient decreases asymptotically. Both coefficients convection and radiation, match at the temperature difference value of 1.7 K, approximately. For temperature differences of 2.5 K or higher, the radiation coefficient represents at least 60% of the total heat transfer coefficient. The high influence of the radiation phenomena can be explained because of the large surface emissivity value of the outer cylindrical surface, $\varepsilon = 0.92$. These results show that, for tanks similar to the one considered in this research, the radiation heat transfer cannot be neglected.

4.3. Transient cooling process

As was previously described, the cooling process begins when the electric heater is turned off because the water temperature at the middle of the tank has reached the set value of 353.15 K (80 ºC) and finishes when the water temperature in the tank is below 313.15 K (40 ºC). This process is longer than a day and, in consequence, the process is directly affected by the ambient temperature's natural cyclic behaviour in the laboratory.

Figure 5 shows the local convection and radiation heat transfer coefficients as a function of the outer surface-surrounding air temperatures difference. It can be observed that, in conjunction with results observed for the heating process, all experimental convection coefficients data

could be reasonably represented as an asymptotical function. Again, the convection coefficients higher values were appreciated at lower temperature differences.

On the other hand, in figure 5 it can be observed that the radiation coefficients shown tend to remain constant during the process with a value around of 5 $W \cdot m^{-2} \cdot K^{-1}$, approximately. It is important to point out that both convection and radiation coefficients, except for the special situation mentioned above, showed the same order of magnitude. This means that, if the emissivity value of the outer surface is large, the radiation phenomena cannot be neglected in this kind of study, as is the case of the tank evaluated in this research.

5. CORRELATION FOR TRANSIENT LAMINAR FREE CONVECTION HEAT TRANSFER

From the experimental results depicted in figures 4 and 5 it can be observed that, for transient heating and cooling processes, when the outer surface-surrounding air temperature difference tends towards zero, the local convection heat transfer coefficient tends to rise a lot. In this case, the radiation coefficient tends to be a small part of the total heat transfer coefficient, even if the emissivity of the outer surface is near to one. Those results indicate that for low temperature differences neither convection nor radiation are the heat transfer dominant modes. In this stage of the transient process, the heat seems to be transferred mainly by conduction between the outer cylindrical surface and the surrounding air, which acts as a semi-infinite medium.

Taken into account a step change in the surface temperature, the analytical solution of the semi-infinite region yields the Eq. (13) for the heat flux.

$$q''(t) = \frac{k \cdot (T_S(t) - T_\infty)}{\sqrt{\pi \cdot \alpha \cdot t}} \qquad (13)$$

The heat transfer flux from the surface to the semi-infinite region, i.e. the surrounding air, can be expressed as transferred by convection according to the Eq. (14).

$$q''(t) = h(t) \cdot (T_S(t) - T_\infty) = \frac{k \cdot (T_S(t) - T_\infty)}{\sqrt{\pi \cdot \alpha \cdot t}} \qquad (14)$$

Then the convection heat transfer coefficient is given in Eq. (15).

$$h(t) = \frac{k}{\sqrt{\pi \cdot \alpha \cdot t}} \qquad (15)$$

The previous equation can be expressed as a function of the local Nusselt number, as is shown in Eq. (16).

$$Nu(t)_x = \frac{x}{\sqrt{\pi \cdot \alpha \cdot t}} \qquad (16)$$

Taking into account the definition of the Fourier number (Eq. 17), the equivalent Nusselt number can also be written as a function of the Fourier Number in Eq. (18).

$$Fo = \frac{\alpha \cdot t}{x^2} \qquad (17)$$

$$Nu = \frac{1}{\sqrt{\pi \cdot Fo}} \qquad (18)$$

Moreover, the effects of the temperature raise due to conduction similar to the semi-infinite region can also be expressed in Eq. (19) as a correlation of the Nusselt number as a function of the Rayleigh number ($Nu = f(Ra^{1/4})$).

$$Nu = \frac{1}{\sqrt{\pi \cdot t}} \cdot \sqrt[4]{\frac{x \cdot Cp \cdot \mu}{g \cdot \beta \cdot k \cdot (T_S - T_\infty)}} \cdot Ra^{1/4} \qquad (19)$$

The above equation permits the calculation of the Nusselt number as a function of the Rayleigh number by means of a correlation similar to the natural convection correlations. Therefore, Eq. (19) allows taking into account the effect of conduction phenomenon in transient natural convection processes. The above equation can be rearranged in Eq. (20) by avoiding the effect of the Rayleigh number and evaluating the time and the temperature difference effects.

$$\frac{Nu}{Ra^{1/4}} = t^{-0.5} \cdot (T_S - T_\infty)^{-0.25} \cdot \sqrt[4]{\frac{x \cdot Cp \cdot \mu}{g \cdot \beta \cdot k \cdot \pi^2}} \qquad (20)$$

Then, the above equation shows that the Nu-Ra ratio depends on time with an exponent of (-0.5) and of temperature difference with an exponent of (-0.25). It is noteworthy that in steady-state natural convection the Nu-Ra ratio remains constant. Therefore, the above equation introduces the effect of time and consequently the transient nature in the transient natural convection process.

Results in Maranzana et al. [10] clearly show that the transient heat transfer is higher than the steady one while the temperature difference is changing. The time dependence shown was a power of -1 and not -0.5 as obtained from the semi-infinite conductive model. However, in processes where the temperature change takes longer, the significance of time is not well accounted for as a function of time. Moreover, it is more adequate to account for the temperature difference change than for time dependence. The temperature difference depends on time; the effect of time can be introduced by means of its influence on the temperature difference and consequently the time dependence in the equation is avoided. Therefore, the idea is to find a correlation based on the general form indicated below taking into account the relationship between the temperature difference and time.

If the temperature difference is proportional to the time, the temperature difference can be expressed in Eq. (21).

$$(T_S - T_\infty) = a \cdot t \qquad (21)$$

Then, the time can be expressed as a function of the temperature difference as indicated in Eq. (22).

$$t = \frac{T_S - T_\infty}{a} \qquad (22)$$

Combining Eq. (20) and (22) results Eq. (23).

$$\frac{Nu}{Ra^{1/4}} = a^{0.5} \cdot (T_S - T_\infty)^{-0.75} \cdot \sqrt[4]{\frac{x \cdot Cp \cdot \mu}{g \cdot \beta \cdot k \cdot \pi^2}} \qquad (23)$$

The above equation can be taken as a base to correlate the experimental data obtained in this research. Eq. (23) can also express it in a more generalized way than Eq. (24), which is the test function chosen for the correlation of the experimental data. The local nature of the Nusselt number and the local heat transfer coefficient is reflected by the value of x.

$$\frac{Nu_x}{Ra_x^{1/4}} = c1 \cdot (T_S - T_\infty)^{n1} \cdot \sqrt[4]{\frac{x \cdot Cp \cdot \mu}{g \cdot \beta \cdot k \cdot \pi^2}} \qquad (24)$$

The constant (c1) and the exponent (n1) in the above equation depend on the relationship between temperature difference variations and time. Both constants must be obtained from experimental data.

Figure 6 shows the experimental data for the heating process evaluated as well as data for Eq. (24) with the exponent value (exp) -0.9 and the constant value (CTE) 2.7. In addition, data from the correlation of Churchill and Usagi [20] for constant wall temperature, Eq. (25), data from correlation developed by Churchill [7] for interpolation between pure conduction and steady-state convection, Eq. (26), and data for steady-state free convection correlations Eqs. (11) and (12) are included.

$$\frac{Nu_x^{20}}{Ra^5} = \left(\frac{1}{\pi \cdot t}\right) \cdot \left[\frac{Cp \cdot \mu \cdot x}{g \cdot \lambda \cdot \beta \cdot (T_S - T_\infty)}\right]^5 + \left\{\frac{\left[1 + \left(\frac{0.492}{Pr}\right)^{9/16}\right]^{-4/9}}{1 + \left(\frac{1.35}{t}\right)^8 \cdot \left[\frac{Cp \cdot \mu \cdot x}{g \cdot \lambda \cdot \beta \cdot (T_S - T_\infty) \cdot \left[1 + \left(\frac{0.437}{Pr}\right)^{9/16}\right]^{-16/9}}\right]^4}\right\}^{20} \qquad (25)$$

$$Nu_x^6 = \left(\frac{\pi \cdot \rho \cdot Cp \cdot x^2}{4 \cdot k \cdot t} \right)^3 + 0.1005 \cdot \left(Ra_x \cdot \left[1 + \left(\frac{0.437}{Pr} \right)^{9/16} \right]^{-16/9} \right)^{3/2} \quad (26)$$

From figure 6, experimental data reveals that the highest local Nusselt number values were obtained for lower temperature differences (lower local Rayleigh numbers) at each measurement position. As the temperature difference increases (local Rayleigh number increments), the local Nusselt number decreases and tends towards the steady-state behaviour represented for data from Eqs. (11) and (12).

It should also be pointed out that the local Nusselt number is well qualitatively represented by data from correlation developed in this research, Eq. (24), for the three heating processes evaluated, as can be appreciated in figure 6. An average deviation from -13.3% to +17% at three heights evaluated was observed for heating powers of 2.2 and 4 kW. The worst results were obtained in the process using the highest heating power of 12 kW, which corresponds to the fastest heating process.

In addition, in figure 6 it can be observed that from a global point of view the well-known correlations included for steady-state and transient behaviours clearly under estimate the local Nusselt number during the development of the process. In those cases, the average deviation observed varied from -79.3% (Churchill and Chu-Eq. (12) , x_1, 12 kW) to -30.5% (Churchill-Eq. (26), x_2, 4 kW).

On the other hand, data from the Churchill and Usagi correlation (Eq. 25) showed a different result as seen in figure 6. At each height considered, this correlation under estimated the local Nusselt number for the lower local Rayleigh numbers while an overestimation of the local Nusselt number for the higher local Rayleigh numbers, was observed. In this case, the average deviation was from -71% at x_3 position and heating power of 2.2 kW, to +24.9% at x_2 position and heating power of 4 kW.

Regarding the cooling process, figure 7 shows experimental data of local Nusselt numbers as well as data from proposed correlation Eq. (24), and from well-known correlations Eqs. (11), (12), (25) and (26). As was mentioned before, the experimental data was collected during five continuous days. In figure 7 no clear tendency can be observed from the experimental data collected. However, it can be observed at each measurement position that, when the temperature difference falls (reduction of the local Rayleigh number), the experimental local Nusselt number tends to rise moving away from the steady-state condition represented in data from Eqs. (11) and (12).

In order to make comparisons between experimental and correlated data, representative local Nusselt and Rayleigh average values were calculated daily for each cooling process. These representative “1 day average experimental data” values, and data from well-known correlations Eqs. (11), (12), (25) and (26) are depicted in figure 8. It can be appreciated that the local Nusselt number is also well represented qualitatively by data from correlations developed in this research (Eq. 24) for the three evaluated heating processes. Except for the Churchill and Usage correlation, the well-known correlations underestimate the local Nusselt number again. Likewise, the same behaviour observed in heating processes in the Churchill and Usagi correlation’s data, was observed in this case. It was also observed that at each height for lower local Rayleigh numbers, this correlation under estimates the local Nusselt number, and for higher local Rayleigh numbers the local Nusselt number was over estimated.

The maximum deviations of the correlations considered compared to “1 day average experimental data” are:

- for Churchill and Ozoe correlation (Eq. 11): from -79.5% to -0.6%;
- for Churchill an Chu correlation (Eq. 12): from -80.1% to -10.7%;
- for Churchill and Usagi correlation (Eq. 25): from -55.4% to 76.3%;
- for Churchill correlation (Eq. 26): from -75.1% to +20.4%;
- for proposed correlation (Eq. 24): from -23.6% to 33.2%.

6. CONCLUSIONS

Experimental data of local convection heat transfer coefficients obtained from a full-scale cylindrical tank for heating and cooling experiments reveals that the transient convection coefficients are different from the values calculated from the well-known correlations. Therefore, it highlights that significant errors can occur in practice if the transient nature of these processes is not accounted for.

In the paper, the experimental apparatus and the calculation procedure used to obtain the experimental data are described. The discrepancies between the experimental data and the values provided by the correlations at disposal in the literature are pointed out.

Experimental results for heating and cooling processes reveal that the transient behaviour of the local convection coefficient is highly dependent on temperature difference evolutions between the outer surface and the surrounding air. Experimental results from all tests show that the $Nu \cdot Ra^{-1/4}$ ratio decreases proportionally in $(T_s-T_\infty)^{-0.9}$.

In addition and taking into account the semi-infinite region theory a new correlation for laminar transient free convection was proposed and compared to experimental results. The proposed correlation showed lower deviation from the experimental data than data provided by well-known correlations obtainable from open literature.

On the other hand, experimental results showed the high influence of the equivalent radiation heat transfer coefficient on the total heat transfer coefficient, due to the high emissivity of the white lacquer outer surface of the tank considered in this research. The radiation heat transfer can not be neglected in this kind of hot water storage tanks.

Data and correlations to calculate transient natural convection coefficients obtainable in textbooks or in more specific open literature, are very scarce. Moreover, the correlations that were found and take into account the transient nature of the processes also provide results quite different from the experimental data. Therefore, more research should be carried out in this area in order to provide the practical engineers with more reliable correlations and calculation tools.

References

[1] F.P. Incropera, D.P. De Witt, Fundamentals of heat and mass transfer, 2nd edition, John Wiley and Sons Inc., New York, USA (1985).

[2] A. Bejan, A.D. Kraus, Heat transfer handbook, John Wiley and Sons Inc., New Jersey, USA (2003).

[3] R. Siegel, Transient free convection from a vertical flat plate, Trans. Am. Soc. Mech. Engrs. 80 (1958) 347–359.

[4] R.J. Goldstein, E.R.G. Eckert, The steady and transient free convection boundary layer on a uniformly heated vertical plate, Int. J. Heat Mass Transfer 1 (1960) 208–218.

[5] B. Gebhart, Transient natural convection from vertical elements, J. Heat Transfer (1961) 61–70.

[6] B. Gebhart, Transient natural convection from vertical elements – appreciable thermal capacity, J. Heat Transfer (1963) 10–14.

[7] S.W. Churchill, Transient, laminar free convection from a uniformly heated vertical plate, Letters in Heat and Mass Transfer 2 (1975) 311-314.

[8] G.F. Hewitt, Heat exchanger design handbook. Part 2. Fluid mechanics and heat transfer. Begell House Inc. U.K (2002).

[9] S.D. Harris, L. Elliott, D.B. Ingham, I. Pop, Transient free convection flow past a vertical flat plate subjected to a sudden change in surface temperature, International Journal of Heat and Mass Transfer 41 (1998) 2311-2322.

[10] G. Maranzana, S. Didierjean, B. Bémy, D. Maillet, Experimental estimation of the transient free convection heat transfer coefficient on a vertical flat plate in air, International Journal of Heat and Mass Transfer 45 (2002) 3413-3427.

[11] T. De Lorenzo, J. Padet, Parametric study of transient free convection heat transfer, International Journal of Heat and Mass Transfer 45 (2002) 2629-2632.

[12] N.H. Saeid, Periodic free convection from vertical plate subjected to periodic surface temperature oscillation, International Journal of Thermal Sciences 43 (2004) 569-574.

[13] A. Shapiro, E. Federovich, Prandtl number dependence of unsteady natural convection along a vertical plate in a stably stratified fluid, International Journal of Heat and Mass Transfer 47 (2004) 4911-4927.

[14] W. Lin, S.W. Armfield, J.C. Patterson, Unsteady natural convection boundary-layer flow of linearly-stratified fluid with Pr<1 on an evenly heated semi-infinite vertical plate, International Journal of Heat and Mass Transfer 51 (2008) 327-343.

[15] A. Mazikowski, K. Chrzanowski, Non-contact multiband method for emissivity measurement, Infrared Physics & Technology 44 (2003) 91–99.

[16] E.W. Lemmon, M.O. McLinden, M.L. Huber, Reference Fluid Thermodynamic and Transport Properties (REFPROP), Version 7.0. National Institute of Standards and Technology (NIST) (2004).

[17] S.W. Churchill, H. Ozoe, A correlation for laminar free convection, J. Heat Transfer 95 (1973) 540-541.

[18] S.W. Churchill, H. Chu, Correlating equations for laminar and turbulent free convection from a vertical plate, International Journal of Heat and Mass Transfer 18 (1975) 1323-1329.

[19] J. Fernández-Seara, F.J. Uhia, J. Sieres, Experimental analysis of a domestic electric hot water storage tank, Part I: Static mode of operation. Applied Thermal Engineering 27 (2007) 129–136.

[20] S.W. Churchill, R. Usagi, A standardized procedure for the production of correlations in the form of a common empirical equation, Ind Eng. Chem. Fundam. 13 (1974) 39-44.

Figures captions

Figure 1. Geometry of the hot water storage tank cylinder and location of the temperature sensors. Dimensions in mm.

Figure 2. Local Nusselt number as a function of local Rayleigh number in steady-state conditions. Experimental and correlations data.

Figure 3. Local convection and radiation heat transfer coefficients as a function of temperature difference. Transient heating process with heating power of 2.2 kW.

Figure 4. Local convection and radiation heat transfer coefficients as a function of temperature difference. Transient heating processes with heating powers of 2.2, 4 and 12 kW.

Figure 5. Local convection and radiation heat transfer coefficients as a function of temperature difference. Transient cooling process.

Figure 6. Local Nusselt number as a function of local Rayleigh number for transient heating processes. Correlations and experimental data.

Figure 7. Local Nusselt number as a function of local Rayleigh number for transient cooling process. Correlations and experimental data.

Figure 8. Representative “1 day average experimental data” local Nusselt number and correlations data as a function of local Rayleigh number for transient cooling process.

Figures

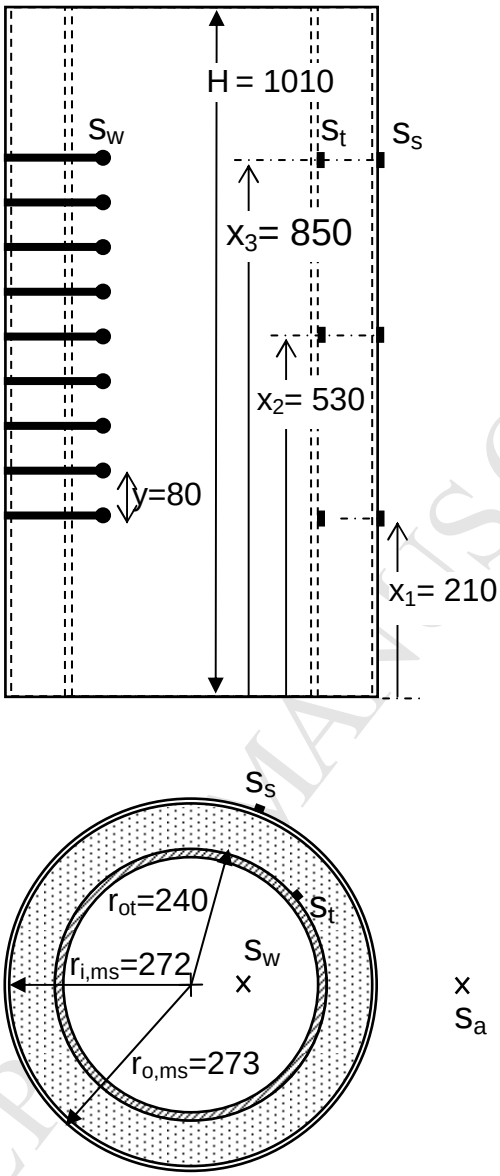

Figure 1

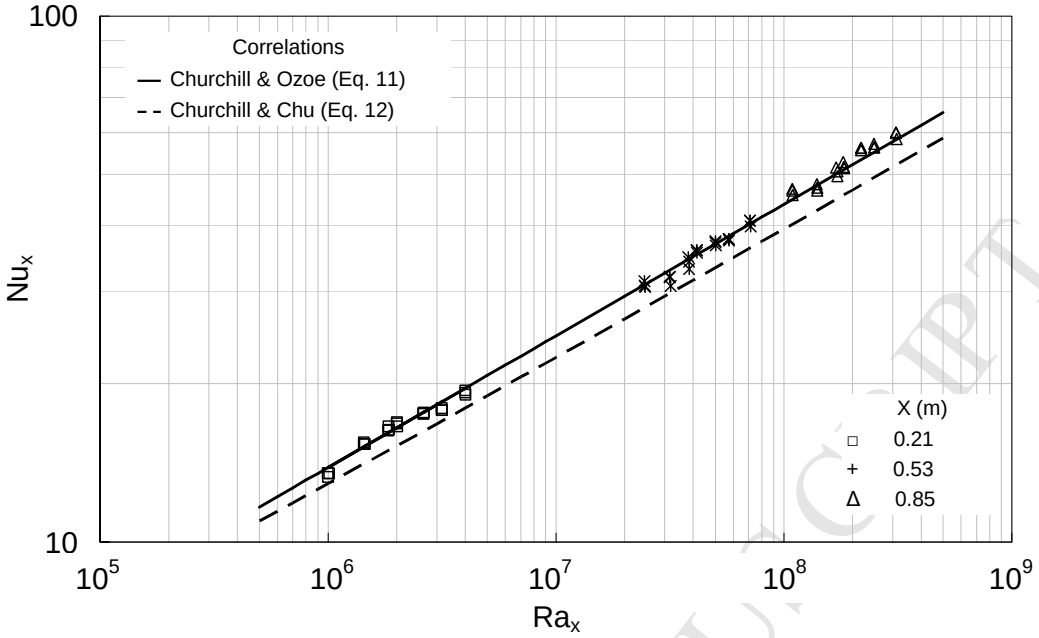

Figure 2

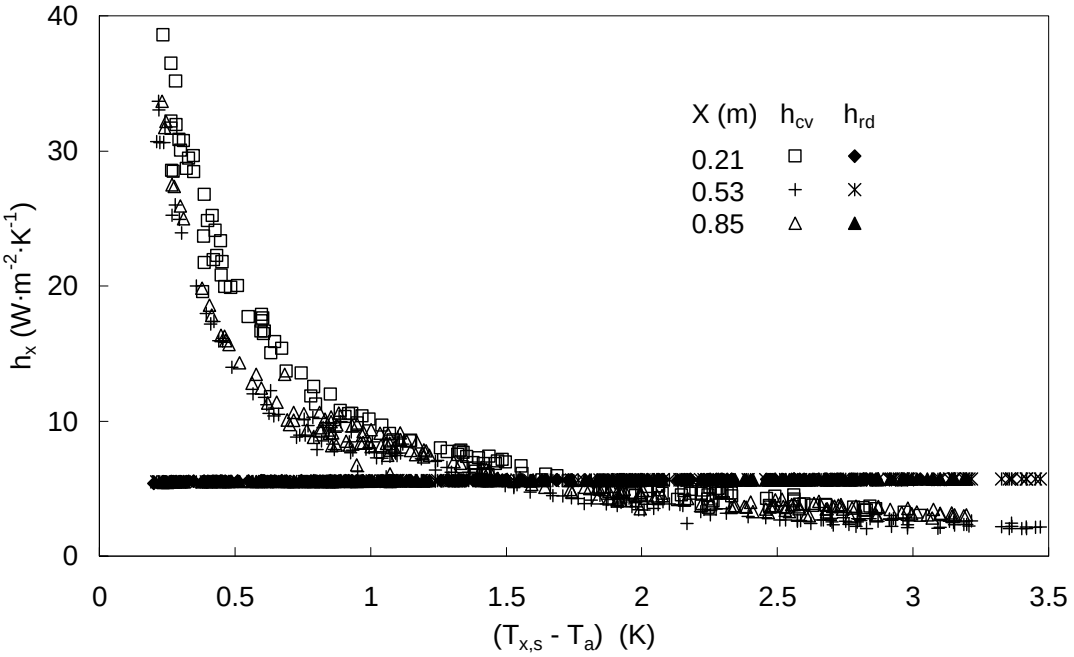

Figure 3

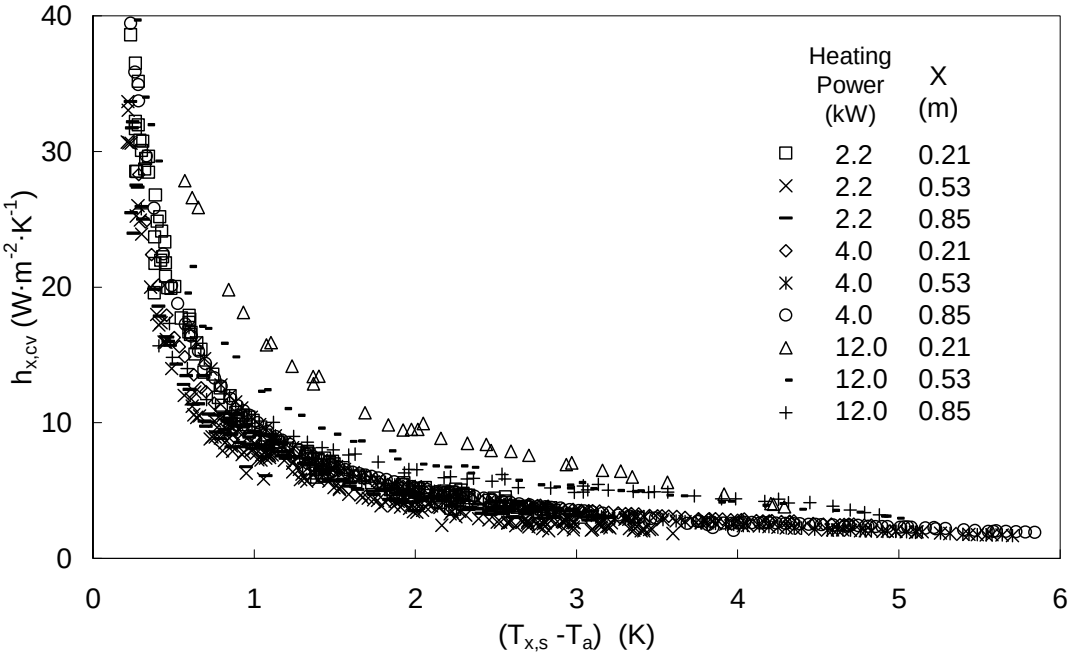

Figure 4

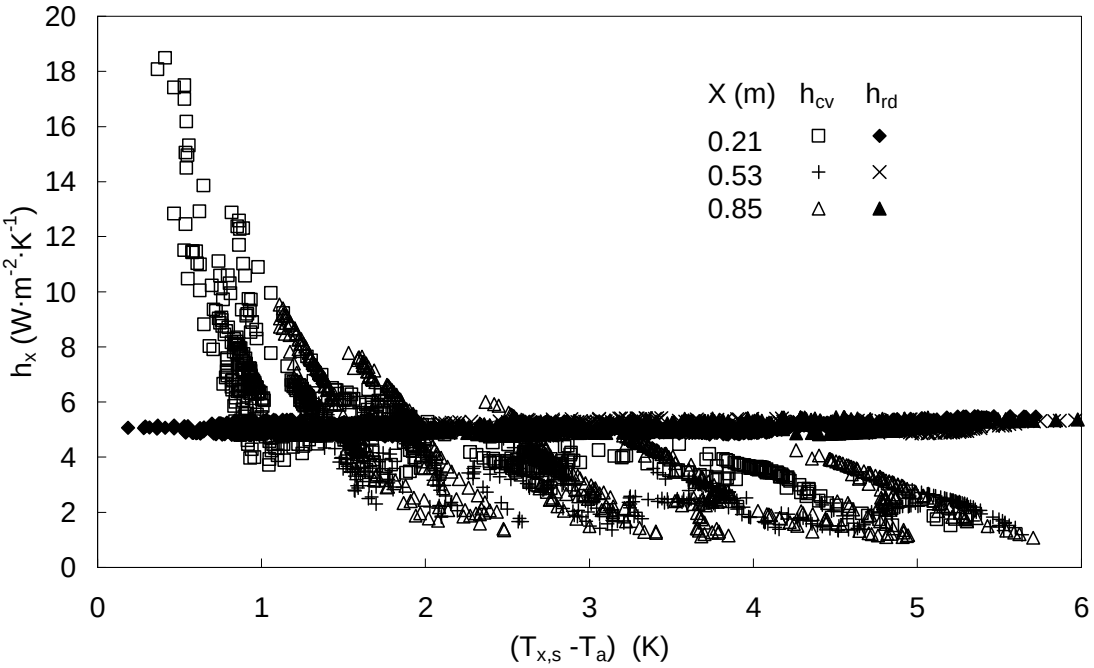

Figure 5

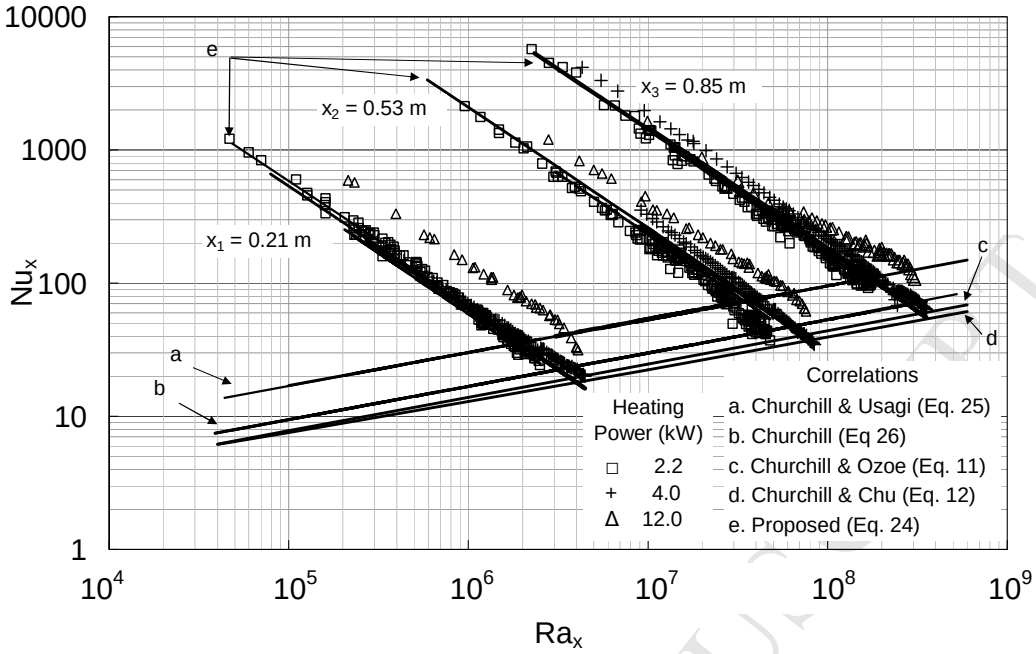

Figure 6

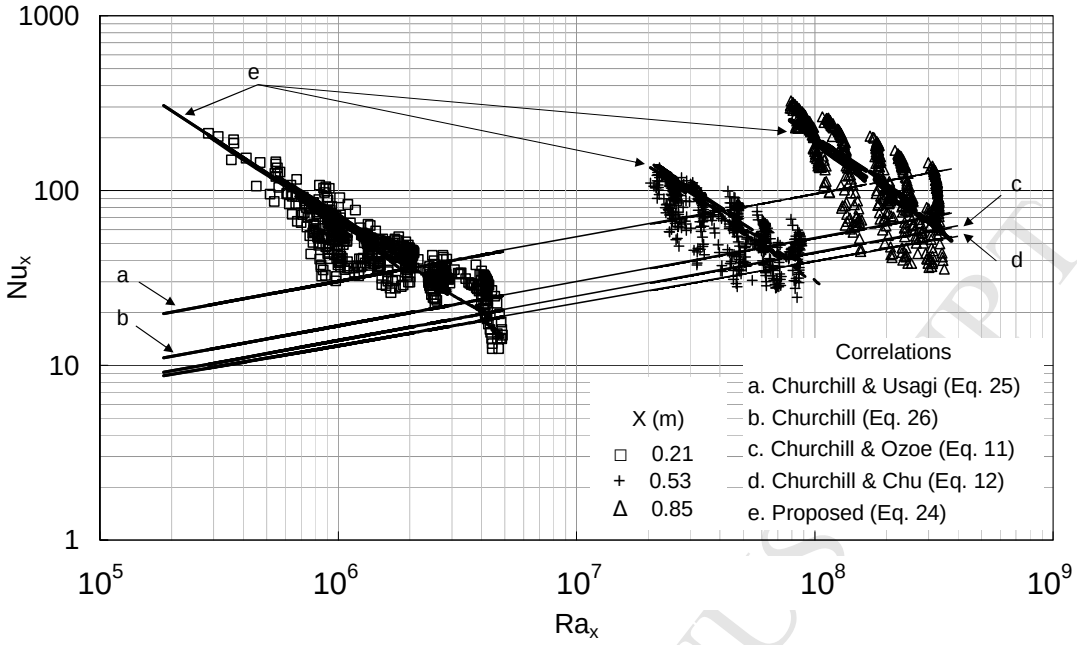

Figure 7

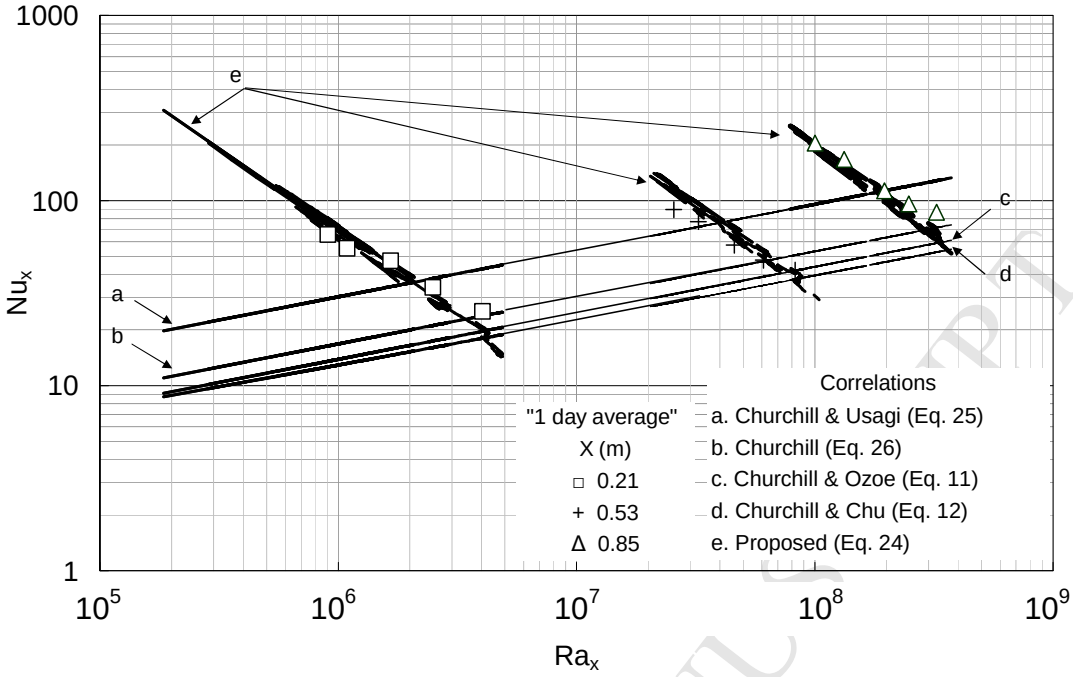

Figure 8